J. Phys. Chem. A **2000,** *104,* 5817−5824

Formation of Two Isomeric C_3HO Radicals from Charged Precursors in the Gas Phase. Potential Interstellar Molecules

Salvatore Peppe, Stephen J. Blanksby, Suresh Dua, and John H. Bowie*

Department of Chemistry, The University of Adelaide, Adelaide, South Australia 5005, Australia

Received: November 30, 1999; In Final Form: April 3, 2000

Theoretical calculations of the C_3HO potential surface at the CCSD(T)/aug-cc-pVDZ//B3LYP/6-31G* level indicate that the three radicals HCCCO, CCCHO, and (cyclo-C_3H)═O are stable, with HCCCO being the most stable of the three. A fourth isomer, CCHCO, is unstable with respect to cyclization to (cyclo-C_3H)═O. Two isomers have been prepared by neutralization of charged precursors, formed as follows: (i) HCCCO, by HC≡C−C(O)−$^+$O(H)(Me) → HC_3O^+ + MeOH, and (ii) C_2CHO, by (a) Me_3SiC≡C−CHO + HO^- → $^-$C≡C−CHO + Me_3SiOH and (b) $^-$C≡C−CH(OH)−C≡CH → $^-$C≡C−CHO + C_2H_2. A comparison of the CR and $^-NR^+$ spectra of ^-C_2CHO indicate that C_2CHO is (partially) rearranging to an isomer that shows significant formation of $CO^{\bullet+}$ in the $^-NR^+$ spectrum of the anion. Ab initio calculations indicate that HCCCO is the product of the isomerism and that a proportion of these isomerized neutrals dissociate to CO and C_2H. The neutral HCCCO may be formed by (i) synchronous rearrangement of C_2CHO and/or (ii) stepwise rearrangement of C_2CHO through (cyclo-C_3H)═O. The second of these processes should have the higher rate, as it has the lower barrier in the rate-determining step and the higher Arrhenius pre-exponential *A* factor.

Introduction

Cumulenes and polycarbon monoxides have been detected in circumstellar envelopes that surround red giant stars and also in dark interstellar molecular clouds.[1−3] Detected cumulenes include a number of C_n ($n = 3$ and 5), C_nH ($n = 2-8$), and C_nH_2 ($n = 2-4$ and 6) molecules.[1−5] In contrast, there has been only limited detection of polycarbon monoxides. The linear species C_2O and C_3O [together with the associated propynal (HC≡C−CHO)] have been detected toward the dark molecular cloud TMC-1,[6,7] while preliminary measurements suggest that C_5O may also be present, but this is yet to be confirmed.[8] Linear C_5O has been synthesized from an anionic precursor.[9] A number of theoretical studies have been devoted to polycarbon monoxides,[10−14] and the photoelectron spectra of C_2O and C_3O have also been determined.[15] The rotational spectra of C_nO ($n = 2-9$) have been detected in pyrolytic decomposition and pulsed discharge nozzle experiments.[16−18]

The aim of the work presented in this paper is to prepare C_3HO neutral radicals from charged precursors and to investigate their stability. Our interest follows from consideration of a number of reports which suggest that the mechanism of formation of the circumstellar molecules C_3O and propynal may be linked via ion−molecule chemistry[19] or by photolysis of the cluster $C_3{}^{\bullet}H_2O$[20−22] and that the reaction $C_3O^{\bullet+} + H_2 \rightarrow C_3HO^+ + H^{\bullet}$ may provide a stellar pathway for the consumption of C_3O.[23] These reports lead us to suggest that C_3HO neutrals, and perhaps ions, may co-occur with C_3O and HC≡C−CHO in the stellar environment.[24]

Experimental Section

All mass spectra were measured using a VG ZAB 2HF mass spectrometer equipped with tandem collision cells between the magnetic and electric sectors. The instrument was used in both the positive ion chemical ionization (PICI) mode and the negative ion chemical ionization (NICI) mode, as appropriate. The MH^+ ion of methyl propiolate was formed using methanol as the protonating agent, and negative ions were formed in the chemical ionization source using either deprotonation of the sample with HO^- or by an S_N2 (Si) reaction between HO^- and a trimethylsilyl derivative ($HO^- + Me_3SiR \rightarrow R^- + Me_3SiOH$).[25] Samples were introduced through the septum inlet (maintained at 100 °C) to a measured pressure of 5×10^{-7} Torr, together with the reagent gas (either methanol for PICI, or water for NICI) at a measured pressure of 1×10^{-5} Torr. The estimated total pressure in the chemical ionization source is 10^{-1} Torr.[26] The ion source temperature was 200 °C, the accelerating voltage was 7 kV, and the slits were fully open to obtain maximum sensitivity. Collisional activation MS/MS experiments were carried out using the magnet to focus and transmit the ion beam under study, the ion beam was intercepted at the first of the tandem collision cells that contained Ar as collision gas at a measured pressure of 1×10^{-6} Torr [reducing the beam transmission to 80% (equivalent to single collision conditions)]. Ionic dissociation products were detected by scanning the electric sector. The same experimental parameters were used for CR experiments,[27,28] except that polarity of the sector voltage was reversed to allow the detection of positive ions, and O_2 was used as the collision gas. Neutralization reionization [$^+NR^+$ (magnet set for transmission of positive ions) or $^-NR^+$ (magnet set for transmission of negative ions)] experiments[29,30] were carried out as for CR experiments. Dioxygen was used as collision gas in both collision cells (pressure measured outside each cell = 1×10^{-6} Torr, 80% beam transmission through collision cells) for $^-NR^+$ experiments. For $^+NR^+$ experiments, benzene was used in the first collision cell, while O_2 was used in the second cell (pressures as for $^-NR^+$ experiments). For both $^-NR^+$ and $^+NR^+$ experiments, the deflector plate between the two collision cells was switched on in order to deflect all ions before they enter the second collision cell.

A. Computational Methods. Geometry optimizations were carried out with the Becke 3LYP method[31,32] using the 6-31G*

10.1021/jp994229g CCC: \$19.00

TABLE 1: Geometries and Energies of Isomers 1−3

	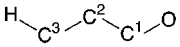 **1**	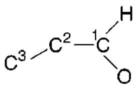 **2**	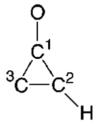 **3**
state	2A′	2A′	2A′
symmetry	C_s	C_s	C_s
energy (hartrees)[a]	−189.51812	−189.45189	−189.49676
rel energy (kcal mol$^{-1)}$	0	51.6	13.4
adiabatic electron affinity (eV)	1.06	3.72	1.9
dipole moment (Debye)[b]	3.49	2.54	3.55
bond length (Å)[b] or angle (deg)			
C^1C^2	1.38	1.44	1.45
C^2C^3	1.23	1.25	1.34
C^1C^3	2.57	2.67	1.46
C^1O	1.19	1.22	1.20
C^1H	3.64	1.10	2.41
C^2O	2.44	2.31	2.55
C^2H	2.29	2.18	1.08
C^3O	3.67	3.55	2.60
C^3H	1.07	3.20	2.36
$C^1C^2C^3$	162.5	162.7	63.0
$C^2C^1C^3$			54.9
C^2C^1O	143.9	119.9	149.2
C^2C^3H	169.0		
HC^1O		122.9	
HC^1C^2			
HC^3C^2			
HC^2C^1			143.9
$C^1C^2C^3O$	0.0	0.0	0.0
$C^1C^2C^3H$	0.0	180.0	0.0

[a] CCSD(T)/aug-cc-pVDZ level of theory including zero point energy (calculated from vibrational frequencies at the B3LYP/6-31G* level of theory and scaled by 0.9804.[34] [b] B3LYP/6-31G* level of theory.

basis within the GAUSSIAN 94[33] suite of programs. Stationary points were characterized as either minima (no imaginary frequencies) or transition states (one imaginary frequency) by calculation of the frequencies using analytical gradient procedures. The minima connected by a given transition structure were confirmed by intrinsic reaction coordinate (IRC) calculations. The calculated frequencies were also used to determine the zero-point vibrational energies, which were then scaled by 0.9804[34] and used as a zero-point energy correction for the electronic energies calculated at this and higher levels of theory. We have previously reported the success of the B3LYP method in predicting geometries of unsaturated carbon chain structures. It was demonstrated previously[35] that this method produced optimized structures, at a low computational cost, that compared favorably with higher level calculations. More accurate energies for the B3LYP geometries were determined with the coupled cluster method, CCSD(T)[36−40] using the Dunning aug-cc-pVDZ basis set.[41,42]

Calculations were carried out using the Power Challenge Super Computer at the South Australian Super Computing Centre (Adelaide).

B. Synthetic Procedures. Methyl propiolate was a commercial sample. 3-Hydroxypenta-1,4-diyne and 3-$^1H_1$-3-hydroxypenta-1,4-diyne were available from a previous study.[35] Trimethylsilyl vinyl ketone[43] and cyclopropenone dimethyl ketal[44] were made by reported methods.

Results and Discussion

Theoretical Studies of Neutral Isomers of C_3HO. If C_3O is converted to propynal by ion molecule reactions in the stellar medium, or if these two molecules are formed from a $C_3{}^{\bullet}H_2O$ cluster, then it is likely that neutrals (and perhaps ions) with the composition C_3HO may also be present in that medium. It has already been reported that $C_3O^{\bullet+}$ reacts with dihydrogen (the most abundant circumstellar molecule) in the laboratory to yield $HCCCO^+$ and $H^{\bullet}$ but that $HCCCO^+$ is stable and does not react further with H_2 to yield ionic products.[19] However, HC_3O^+ could capture an electron to yield the radical $HC_3O^{\bullet}$, and there are other $C_3HO^{\bullet}$ isomers that could be formed from C_3O or $HC{\equiv}C{-}CHO$ or their charged counterparts. There are four isomers of $C_3HO^{\bullet}$ that contain a carbonyl function, viz. HC_3O, C_2CHO, CCHCO, and (cyclo-C_3H)═O. We have investigated the structures and energies of these isomers using theoretical calculations at the CCSD(T)/aug-cc-pVDZ//B3LYP/6-31G* level of theory. These calculations indicate that CCHCO is unstable and undergoes ring closure to yield the cyclic isomer (cyclo-C_3H)═O. The structures of the three stable C_3HO radicals, HC_3O (**1**), C_2CHO (**2**), and (cyclo-C_3H)═O (**3**) are shown in Figure 1: full details of their geometries and energies are listed in Table 1. The geometries of the two neutrals **1**[17,45−47] and **3**[45] have been reported previously. Although all of these studies have shown that **1** has a bent structure (see Figure 1), there are differences in the reported bond lengths and angles of this species.[48] It has also been reported that HC_3O (**1**) is stable with respect to decomposition to CO and $^{\bullet}C_2H$: this process is calculated to be endothermic by 33.6 kcal mol^{-1} at the CCSD(T)/DZP//CISD/DZP level of theory.[45] The structures of the isomers **2** and **3** are unexceptional. Isomer **1** is the global minimum on the neutral potential surface, with the relative energies of **1**−**3** being 0, 41.1, and 12.2 kcal mol^{-1}, respectively, at the CCSD(T)/aug-cc-pVDZ//B3LYP/6-31G* level of theory. The adiabatic electron affinities of **1**−**3** are calculated to be 1.03, 3.76, and 1.90 eV at the CCSD(T)/aug-cc-pVDZ//B3LYP/6-31G* level of theory,[49] and their dipole moments are 3.48,

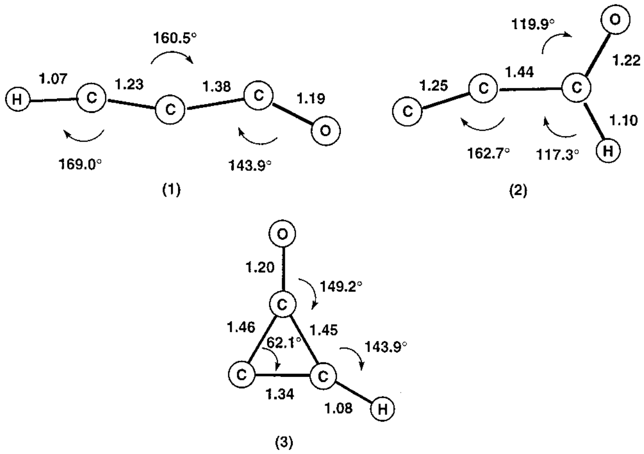

Figure 1. Geometries and relative energies of neutral radicals **1**−**3**.

2.54, and 3.55 D, respectively, at the B3LYP/6-31G* level of theory.

Syntheses of Ionic Precursors. We reasoned that it should be possible to form the neutral radicals **1**−**3** by reactions involving either cationic or anionic precursors. The planned synthetic routes of these precursor ions are shown in eqs 1−6. The simplest precursor to HC_3O (**1**) is the positive ion HC_3O^+, which can be made in the source of the mass spectrometer by loss of methanol from protonated methyl propiolate as shown in eq 1. In contrast, the chosen route to C_2CHO (**2**) is via negative ion $^-C{\equiv}C{-}CHO$. This anionic precursor has been formed by two methods, viz. (a) via the S_N2 (Si) displacement reaction[25] shown in eq 2 and (b) by the reaction sequence shown in eq 3 (the precursor $^-C{\equiv}C{-}CH(OH){-}C{\equiv}CH$ has also been used to synthesize C_2CHC_2[51]). The deuterium analogue ($^-C{\equiv}C{-}CDO$), was prepared similarly (see eq 4).

$$HC{\equiv}C{-}CO{-}^{+}O(H)(Me) \rightarrow HC{\equiv}C{-}C{\equiv}O^+ + MeOH \quad (1)$$

$$Me_3Si{-}C{\equiv}C{-}CHO + HO^- \rightarrow {}^-C{\equiv}C{-}CHO + Me_3SiOH \quad (2)$$

$$HC{\equiv}C{-}H(OH){-}C{\equiv}CH + HO^- \rightarrow {}^-C{\equiv}C{-}CH(OH){-}C{\equiv}CH + H_2O \rightarrow {}^-C{\equiv}C{-}CHO + C_2H_2 + H_2O \quad (3)$$

$$HC{\equiv}C{-}CD(OH){-}C{\equiv}CH + HO^- \rightarrow {}^-C{\equiv}C{-}CDO + H_2O + C_2H_2 \quad (4)$$

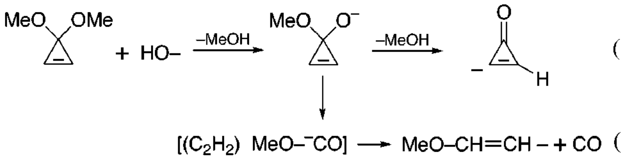

(5)

(6)

$$CH_2{=}CH{-}CO{-}SiMe_3 + O^{\bullet -} \rightarrow [C{=}CH{-}CO{-}SiMe_3]^{\bullet -} + H_2O \rightarrow [CCHCO]^- + Me_3Si^{\bullet} + H_2O \quad (7)$$

$$CH_2{=}CH{-}CO{-}SiMe_3 + O^{\bullet -} \rightarrow CH_2 = {}^-C{-}CO{-}SiMe_3 + HO^{\bullet} \rightarrow [CH_2{=}C{=}C{=}O]^{\bullet -} + (Me_3Si^{\bullet} + HO^{\bullet}) \quad (8)$$

We planned to use deprotonated cyclopropenone as the precursor for (cyclo-C_3H)=O (**3**): the proposed route is shown in sequence 5. The S_N2 reaction between HO^- and the dimethyl ketal of cyclopropenone proceeded as planned, but the product alkoxide anion did not eliminate methanol as expected: instead, carbon monoxide is lost (sequence 6). Sequence 6 seems quite unusual; however, (i) the analogous reaction with the dimethylketal of cyclopropanone is also reported not to form deprotonated cyclopropanone,[52] and (ii) once the ion complex shown in sequence 6 is formed, the subsequent reaction should be facile, since the methoxycarbonyl anion is a good MeO^- donor (the reaction $MeO{-}^-CO \rightarrow MeO^- + CO$ is exothermic by 0.5 kcal mol^{-1} [53]).

Finally, we attempted to form the anionic precursor of unstable CCHCO as shown in sequence 7. If this anion can be formed, charge stripping might proceed through CCHCO to the stable (cycloC_3H)=O (**3**) (as described above). The proposed synthesis of $(CCHCO)^-$ seemed plausible, since $O^{\bullet -}$ is known to react with ethylene to yield $CH_2{=}C^{\bullet -}$ and H_2O.[54] Unfortunately, the reaction shown in sequence 7 does not occur. Instead, $O^{\bullet -}$ reacts exclusively as a base, forming the methylene keten radical anion as shown in sequence 8 (cf. ref 55).

Formation of Neutrals HC_3O and C_2CHO. We have now formed $H{-}C{\equiv}C{-}C{\equiv}O^+$ and $^-C{\equiv}C{-}CHO$, which we hope will capture an electron and lose an electron respectively to form the required neutral radicals HC_3O (**1**) and C_2CHO (**2**). Both of the precursor ions have been formed by soft ionization techniques (in these cases by ion molecule reactions), and as such, they will have little excess energy. We need to know (i) that the precursor ions do not rearrange under the conditions of the neutralization experiments [this will be resolved experimentally (see later)], and we need to know (ii) the minimum excess energy contained by each neutral following formation from the precursor ion (assuming that there is no rearrangement of the precursor ion). This excess energy should give an indication as to whether the neutral is likely to be stable under the conditions of the planned neutralization experiment. The excess energy of formation of each neutral from the ion can be calculated as the difference in energy between the neutral minimum and that of the ion geometry on the ground-state neutral surface: this assumes vertical Franck−Condon overlap of the ion and neutral potential surfaces.[56] It should be stressed that these calculated values are minimum excess energies of formation of the neutral from the ion. They do not include any excess energy that the precursor ion itself may have, or extra energy given to the neutral as a consequence of the collisional process.

The data provided in Tables 1 and 2 show that the structures of each of singlet[57] HC_3O^+ and the radical HC_3O (**1**) are different: the cation is linear but the radical has a bent structure. In contrast, the structures of ^-C_2CHO and C_2CHO (**2**) are very similar. The consequence is that the minimum excess energy of formation of each neutral following the vertical Franck−Condon transition is different. For reduction of HC_3O^+ to HC_3O (**1**), the minimum excess energy of the radical on formation is calculated to be 10.5 kcal mol^{-1}, while for oxidation of $-C_2CHO$ to C_2CHO (**2**) the corresponding minimum excess energy is only 3.2 kcal mol^{-1}. However, both of these energies are modest and should not by themselves be sufficient to induce rearrangement or fragmentation of the neutral. These calculations suggest that neutralization of HC_3O^+ and ^-C_2CHO should produce the stable isomers HC_3O (**1**) and C_2CHO (**2**), respectively.

The collisional-induced (CID) mass spectrum (MS/MS) of $HCCCO^+$ is shown in Figure 2A. Major fragmentations observed in this positive ion spectrum involve losses of $H^{\bullet}$, $HC^{\bullet}$,

TABLE 2: Geometries and Energies of HC_3O^+ and ^-C_2CHO

	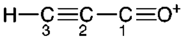 $H-\underset{3}{C}\equiv\underset{2}{C}-\underset{1}{C}\equiv O^+$	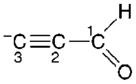
state	1Σ	1A′
symmetry	$C_{\infty v}$	C_s
energy (hartrees)[a]	−189.24969	−189.58876
dipole moment (Debye)[b]	3.92	4.65
bond length (Å)[b] or angle (deg)		
C^1C^2	1.34	1.41
C^2C^3	1.22	1.23
C^1H		1.10
C^3H	1.08	
C^{1O}	1.13	1.21
$C^1C^2C^3$	180.0	174.8
C^2C^1O	180.0	120.1
C^2C^1H		113.7
OC^1H		117.1
$C^1C^2C^3O$	180.0	180.0
$C^1C^2C^3H$	0.0	0.0

[a] CCSD(T)/aug-cc-pVDZ level of theory including zero point energy (calculated from vibrational frequencies at the B3LYP/6-31G* level of thory and scaled by 0.9804.[34] [b] B3LYP/6-31G* level of theory.

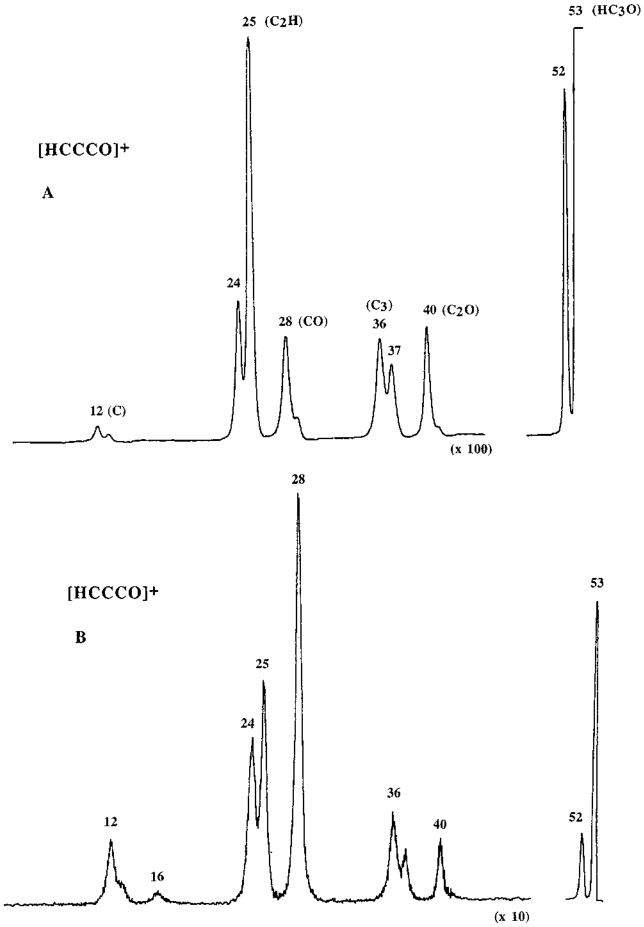

Figure 2. (A) Collision-induced mass spectrum (MS/MS) of HC_3O^+. VG ZAB 2HF instrument. (B) Neutralization/reionization ($^+NR^+$) mass spectrum of HC_3O^+. For experimental conditions see Experimental Section.

$HC_2^•$, and CO from the parent cation, confirming structure $HCCCO^+$. Ions C_3HO^+ have been observed previously in the positive ion spectra of uracil[58] and fumaroyl chloride,[59] and in the reaction between $C_2H_2^{•+}$ and CO in a flowing afterglow tube.[60] We have determined the CID spectra of all three of these ions: they are identical with that shown in Figure 2A, consistent with structure $HCCCO^+$ (we mirrored the flowing afterglow experiment by introducing C_2H_2 and CO into the CI source of the ZAB mass spectrometer and analyzing the source formed $HCCCO^+$ ion). The characteristic neutralization/reionization spectrum[29,30] ($^+NR^+$) of $HCCCO^+$ is shown in Figure 2B: this spectrum is identical with the $^+NR^+$ spectra of the C_3HO^+ ions from fumaroyl chloride, uracil, and the flowing afterglow experiment outlined above. The base peak (*m*/*z* 53) in the $^+NR^+$ spectrum of $HCCCO^+$ corresponds to the parent cation (the recovery signal), with major fragment peaks at *m*/*z* 52 ($C_3O^{•+}$), 28 ($CO^{•+}$), and 25 (C_2H^+). The fragment peak abundances in the $^+NR^+$ spectrum are comparable to those observed in the CID spectrum except for the pronounced increase in *m*/*z* 28 ($CO^{•+}$) compared to *m*/*z* 25 (HC_2^+). This observation is rationalized as follows. The first collision in the $^+NR^+$ experiment leads to both neutralization and fragmentation processes. Therefore, neutrals from parent and fragment ions (from CID pathways) will be transmitted when the charged species are deflected. The CID mass spectrum of $HCCCO^+$ shows that the major fragmentation pathways are $HC_3O^+ \rightarrow C_3O^{•+} + H^•$ and $HC_3O^+ \rightarrow HC_2^+ + CO$. Possible fragmentation processes of $HCCCO^+$, together with associated thermochemical data are summarized in Table 3. The observed fragmentation processes correspond to the least endothermic decomposition channels of $HCCCO^+$ (Table 3). It follows that a significant proportion of the neutral beam must consist of C_3O and CO: these will be reionized together with parent $HCCCO^•$ to contribute to the $^+NR^+$ spectrum (the contribution from neutral fragments is called N_fR[61]). This rationale is favored over direct decomposition of neutral $HCCCO^•$ for the following reason. Some possible decompositions of $HCCCO^•$, together with their thermochemistries are listed in Table 3. The most favorable process, $HC_3O^• \rightarrow HC_2^• + CO$, is endothermic by 34 kcal mol^{-1} (Table 3; see also ref 45). Since the ionization energies of $HC_2^•$ and CO are 11.6 and 14.0 eV, respectively (see also Table 3), it follows that if the neutral decomposition is a major process then the $^+NR^+$ spectrum should show a more pronounced peak at *m*/*z* 25 (HC_2^+) than at *m*/*z* 28 ($CO^{•+}$). The contrary is observed experimentally. We conclude that $HCCCO^•$ is stable for the duration of the NR experiment (ca. 10^{-6} s).

The CR and $^-NR^+$ spectra of $^-C{\equiv}C{-}CHO$ are shown in Figure 3, with the corresponding spectra of the deuterated analogue $^-C{\equiv}C{-}CDO$ listed in Table 4. Major peaks in the CR spectrum (Figure 3A) correspond to losses of $H^•$, C_2, and $^•CHO$ from the parent cation. The first two of these processes are exothermic, while the third (the loss of $CHO^•$) is endothermic by only 33 kcal mol^{-1}. Analogous processes can be seen in the corresponding spectrum of $^-C{\equiv}C{-}CDO$ (Table 4)], in accord with the bond connectivity of the precursor anion and indicating that it does not rearrange upon collisional activation. The $^-NR^+$ spectra of $^-C{\equiv}C{-}CHO$ (Figure 3B) and $^-C{\equiv}C{-}CDO$ (Table 4) exhibit the same peaks as those observed in the corresponding $^-CR^+$ spectra. The losses of $H^•$ and C_2 from C_2CHO^+ are expected, since these processes are exothermic (Table 3). Although these peaks are observed, the $^-NR^+$ spectrum of $^-C{\equiv}C{-}CHO$ (Figure 3B) is quite different from the $^+NR^+$ spectrum of $HCCCO^+$ (Figure 2B). Peaks at *m*/*z* 25 (− CO) and *m*/*z* 28 (− $^•C_2H$) are more abundant in the $^-NR^+$ than in the CR spectrum. In addition, the abundances of peaks in the $^-NR^+$ spectrum are influenced by the pressure of dioxygen in the first collision cell (the cell in which charge stripping of the precursor anion to the neutral is effected). An increase in the pressure of O_2 increases the abundances of the peaks at *m*/*z* 25 and 28, with the increase in *m*/*z* 28 being the more pronounced.

TABLE 3: Thermochemical Data for Decompositions of C_3HO Cations and Neutrals

cation process	ΔH (kcal mol^{-1})	neutral process	ΔH (kcal mol^{-1})
$HCCCO^+ \rightarrow CCCO^{\bullet+} + H^\bullet$	120	$HCCCO^\bullet \rightarrow CCCO + H^\bullet$	66
$HCCCO^+ \rightarrow HCCC^{\bullet+} + O^\bullet$	210	$HCCCO^\bullet \rightarrow HCCC^\bullet + O$	174
$HCCCO^+ \rightarrow HCC^\bullet + CO^{\bullet+}$	198	$HCCCO^\bullet \rightarrow HCC^\bullet + CO$	34[45]
$HCCCO^+ \rightarrow HCC^+ + CO$	142		
$CCCHO^+ \rightarrow CCCO^{\bullet+} + H^\bullet$	−88	$CCCHO^\bullet \rightarrow CCCO + H^\bullet$	24
$CCCHO^+ \rightarrow CCC^{\bullet+} + HO^\bullet$	65	$CCCHO^\bullet \rightarrow CCC + HO^\bullet$	99
$CCCHO^+ \rightarrow CHO^+ + CC$	−42	$CCCHO^\bullet \rightarrow CHO^\bullet + CC$	104
$CCCHO^+ \rightarrow CC^{\bullet+} + CHO^\bullet$	33		

[a] ΔH values are determined from the following thermochemical data [$\Delta H^o{}_f$ (kcal mol^{-1}), ionization energy (eV)]. HC_3O^+ (232[a]), $HC_3O^\bullet$ (64,[c] 7.3[b]), C_2CHO^+ (440[c]), $C_2CHO^\bullet$ (106,[c] 14.5[b]), $C_3O^{\bullet+}$ (300[a]), $C_3O^\bullet$ (78,[a] 9.6[c]), HC_3^+ (383[f]), $HC_3^\bullet$ (178,[c] 8.9[c]), $C_3^{\bullet+}$ (496[c]), C_3 (196,[d] 13.0[d]), HC_2^+ (401[c]), $HC_2^\bullet$ (133,[d] 11.6[d]), $CO^{\bullet+}$ (297[d]), CO (−26,[d] 14.0[d]), HO^+ (310[c]), $HO^\bullet$ (9,[d] 13.0[d]). [a] From ref 62. [b] From theoretical calculations presented in this paper (see Tables 1 and 2); also $HC_3O^- = 189.55699$ and $C_2CHO^+ = -189.05500$ hartrees [at the CCSD(T)/aug-cc-pVDZ level of theory (calculated from vibrational frequences at the B3LYP/6-31G* level of theory and scaled by 0.9804[34])]. [c] From combination of thermochemical data presented above. [d] From the NIST database.[63] [e] From ref 64. [f] Estimated from the proton affinity of C_3: $PA(C_3) = 184$ kcal mol^{-1}.[65]

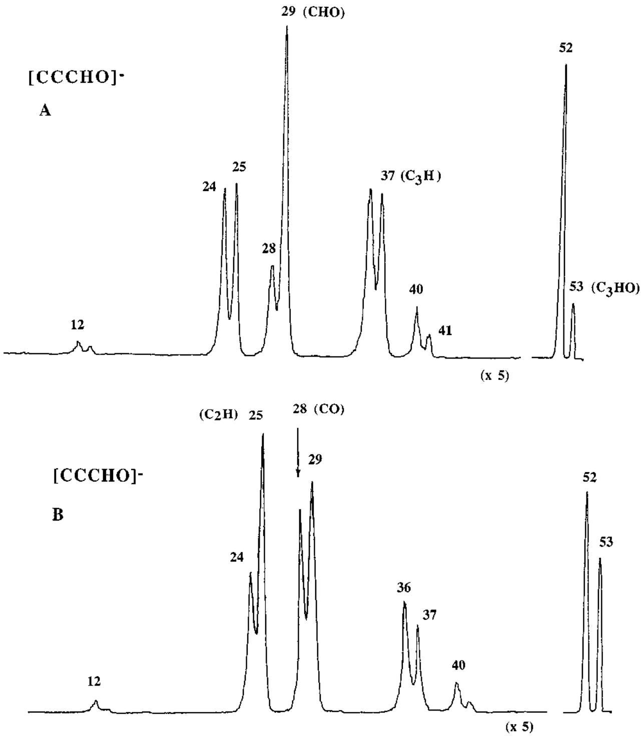

Figure 3. (A) Charge reversal (CR) mass spectrum (MS/MS) of ^-C_2CHO. (B) Neutralization/reionization ($^-NR^+$) mass spectrum of ^-C_2CHO. For experimental conditions see Experimental Section.

TABLE 4: CR and $^-NR^+$ Mass Spectra of $^-C{\equiv}C{-}CDO$ [*m/z* (Relative Abundance)]

charge reversal (CR)	peak composition	neutralization/ reionization ($^-NR^+$)
54(46)	C_3DO^+	54(100)
52(100)	$C_3O^{\bullet+}$	52(98)
42(2)	C_2DO^+	42(4)
40(3)	$C_2O^{\bullet+}$	40(7)
38(14)	C_3D^+	38(15)
36(12)	$C_3^{\bullet+}$	36(14)
30(21)	CDO^+	30(20)
28(8)	$CO^{\bullet+}$	28(12)
26(13)	C_2D^+	26(31)
14(1)	CD^+	14(1)
12(1)	$C^{\bullet+}$	12(1)

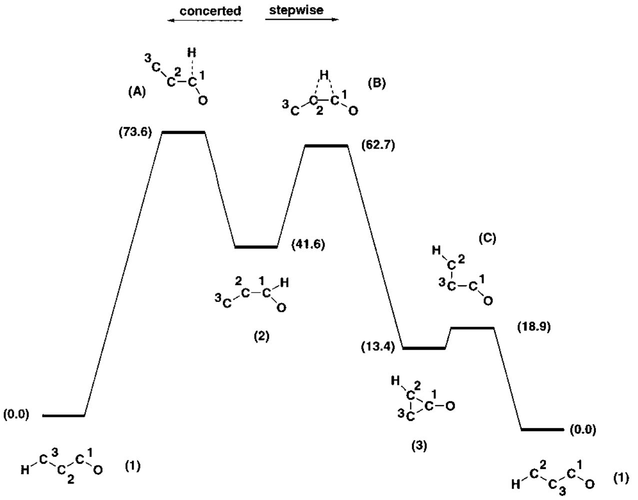

Figure 4. Concerted and stepwise rearrangements of C_2CHO (**2**) to HC_3O (**1**). CCSD(T)/aug-cc-pVDZ//B3LYP/6-31G* level of theory. Relative energies (kcal mol^{-1}) in relation to (**1**) (0.0 kcal mol^{-1}). Full data for neutrals: see Figure 1 and Table 1. Data for transition states A−C: see Table 5.

We conclude that charge stripping of $^-C{\equiv}C{-}CHO$ does produce C_2CHO (**2**) but that the charge-stripping process is particularly sensitive to the pressure of collision gas, with collision-induced vertical oxidation producing a proportion of neutrals with sufficient excess energy to cause them to rearrange to another isomer. The isomerization produces a neutral whose positive ion spectrum is dominated by peaks corresponding to charged CO and $^\bullet C_2H$. This isomerization must involve H migration: the most likely product would seem to be $HCCCO^\bullet$ (**1**), but (cyclo-C_3H)=O (**3**) must also be considered in this context. Since we have been unable to prepare (**3**), the possible rearrangements of (**2**) have been investigated using computational chemistry.

Theoretical Studies of the Rearrangement of Neutral CCCHO. Calculations of possible rearrangements of radical C_2CHO have been investigated at the CCSD(T)/aug-cc-pVDZ//B3LYP/6-31G* level of theory. There are two competitive rearrangements of C_2CHO: these are summarized in Figure 4. Structural and energy data for the three isomers **1**−**3** are shown in Figure 1 and Table 1; the data for the three transition states A−C are recorded in Table 5. The relative energy data shown in Figure 4 conform to the values listed earlier in the text; i.e., HC_3O (energy designated as 0.0 kcal mol^{-1}) is the global energy minimum on the neutral potential surface.

There are two isomerization pathways for C_2CHO (**2**), both terminating with the formation of the stable isomer HC_3O (**1**). The first rearrangement is a synchronous reaction in which the C_1 hydrogen transfers, via four-membered transition state A, to form HC_3O directly. The barrier for this reaction is computed as 32.0 kcal mol^{-1} at the level of theory used. The second isomerization is a stepwise sequence in which the rate determin-

TABLE 5: Geometries and Energies for Transition States A−C (see Figure 4)

	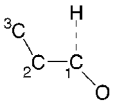 A	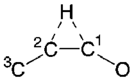 B	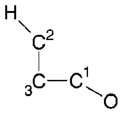 C
state	2A′	2A′	2A′
symmetry	C_s	C_s	C_s
energy (hartrees)[a]	−189.40092	−189.41813	−189.48794
rel. energy (kcal mol^{-1})	73.5	62.7	18.9
bond length (Å)[b] or angle (deg)			
C^1C^2	1.39	1.32	
C^1C^3			1.38
C^2C^3	1.32	1.32	1.34
C^1O	1.19	1.18	1.16
C^1H	1.28	1.38	
C^2H			1.09
$C^1C^2C^3$	92.7	176.7	
$C^1C^3C^2$			85.0
C^2C^1O	150.8	170.8	
C^3C^1O			172.6
HC^1O	113.5		
HC^1C^2	95.7		
HC^2C^3		119.8	137.7
HC^2C^1		63.4	
$C^1C^2C^3O$	0.0	0.0	
$C^1C^2C^3H$	180.0	180.0	
$C^1C^2C^3O$			0.0
$C^1C^2C^3O$			0.0

[a] CCSD(T)/aug-cc-pVDZ level of theory including zero point energy (calculated from vibrational frequencies at the B3LYP/66-31G* level of theory and scaled by 0.9804[34].) [b] B3LYP/6-31G* level of theory.

ing first step involves 1,2 H transfer through transition state B over a barrier of 21.3 kcal mol^{-1}. This reaction should form $^{\bullet}$CCHCO, but this species is unstable and immediately cyclizes to form (cyclo-C_3H)═O (**3**). Isomer **3** is formed with 50.4 kcal mol^{-1} of excess energy in this reaction sequence and it specifically ring opens via transition state C to form HC_3O (**1**). What is not resolved is which of the processes shown in Figure 4 is the more likely? An interesting feature of these two mechanisms is that the carbon chain remains intact during the synchronous isomerization but rearranges for the stepwise process (see Figure 4). In principle, if we label the precursor anion with ^{13}C at either positions 2 or 3 we should be able to differentiate between these two mechanisms. Unfortunately, there is no suitable fragmentation in the $^{-}NR^{+}$ spectrum (Figure 3B) that we believe could be used unequivocally as a mechanistic probe in this regard, so we have not undertaken this labeling study.

Both of the rearrangement mechanisms require rearranging $^{\bullet}C_2CHO$ to have gained excess energy during the collision-induced neutralization process, since the minimum excess energy derived from the vertical Franck−Condon oxidation is only 3.2 kcal mol^{-1} (see earlier). There are two factors controlling the relative rates of these isomerization processes, viz. (i) the relative barriers to the transition states in the rate-determining steps of the reactions and (ii) the relative Arrhenius factors of both processes. As far as the barriers are concerned, the stepwise process is favored by 10.8 kcal mol^{-1}.

We can estimate the relative Arrhenius pre-exponential factors of the two processes by determining the relative vibrational partition functions for the two transition states. We have described this method in detail previously[66](see also ref 67). The data are recorded in Table 6. The value of the vibrational partition function for transition state A (Figure 4) is 1.55, whereas that for B (Figure 4) is 2.24. Therefore, the stepwise process shown in Figure 4 is favored both by the smaller barrier to the transition state in the rate-determining step and by a larger Arrhenius factor.

TABLE 6: Vibrational Partition Functions for Transition States A and B (Figure 4)

A		B	
frequency	Q'_{vib}	frequency	Q'_{vib}
302	1.3025	214	1.5524
474	1.1124	295	1.3159
696	1.0359	597	1.0591
762	1.0258	784	1.0231
1122	1.0044	918	1.0119
1499	1.0007	1595	1.0005
1688	1.0003	1670	1.0003
1936	1.0001	2205	1.0000
total	1.548	total	2.242

Finally, the HC_3O products of the reaction sequence shown in Figure 4 could have minimum formation energies of up to 62.6 kcal mol^{-1} unless they are de-energized by either collision or radiation[68] in the collision cell. It may be, therefore, that some of the HC_3O neutrals formed in the isomerization process have sufficient energy to decompose to yield CO and HC_2 (a process that is endothermic by 33.6 kcal mol^{-1} [45]).

In conclusion, a consideration of both experimental and theoretical evidence indicates that we have formed $HC_3O^{\bullet}$ from HC_3O^{+} and $C_2CHO^{\bullet}$ from $^{-}C_2CHO$. Under the collision conditions used, some of the initially formed C_2CHO radicals rearrange to $HC_3O^{\bullet}$ [a reaction more favorable than simple cleavage of C_2CHO (see Table 3 and compare with Figure 4)], and it is likely that some of these energized HC_3O radicals decompose to yield CO and $^{\bullet}C_2H$.

Acknowledgment. This project was funded by the Australian Research Council. S.D. and S.P thank the ARC for a research associate stipend and a Ph.D. scholarship, respectively.

Supporting Information Available: Unscaled harmonic frequencies (in cm^{-1}) and infrared intensities (in km mol^{-1}) for HC_3O neutral (**1**) (Table S1), C_2CHO neutral (**2**) (Table S2), and (cyc-C_3H)=O neutral (**3**) (Table S3). Dipole moments and rotational constants for the ground states of the three stable C_3HO neutrals, the HC_3O^+ cation, and the C_2CHO^- anion at the B3LYP/6-31G* level of theory (Table S4). This material is available free of charge via the Internet at http://pubs.acs.org.

References and Notes

(1) Olofsson, H. In *Molecules in the Stellar Environment, Lecture Notes in Physics*; Jorgenson, O. G., Ed.; Springer: Heidelberg, 1994; pp 114−133 (see also references cited therein).

(2) Bernath, P. F.; Hinkle, K. H.; Keady, J. J. *Science* **1989**, *244*, 562. Hinkle, K. H. In *Molecules in the Stellar Environment, Lecture Notes in Physics*; Jorgenson, O. G., Ed.; Springer: Heidelberg, 1994; pp 99−114 (see also references cited therein).

(3) Blanksby, S. J.; Bowie, J. H. *Mass Spectrom. Rev.* **1999**, *18*, 131.

(4) Omont, A. In *Molecules in the Stellar Environment, Lecture Notes in Physics*; Jorgenson, O. G., Ed.; Springer: Heidelberg, 1994; pp 135−138 (see also references therein).

(5) Smith, D.; Spanel, P. *Mass Spectrom. Rev.* **1995**, *14* , 255 and references therein.

(6) Ohishi, M.; Suzuki, H.; Ishikawa, S.; Yamada, C.; Kanamori, H.; Irvine, W. M.; Brown, R. D.; Godfrey, P. D.; Kaifu, N. *Astrophys. J.* **1991**, *380*, L39.

(7) Matthews, H. E.; Irvine, W. M.; Friberg, P.; Brown, R. D.; Godfrey, P. D. *Nature* **1984,** *310*, 125.

(8) Turner, B. E. In *Chemistry and Spectroscopy of Interstellar Molecules;* Bohme, D. K., Ed.; University of Tokyo Press: Tokyo, 1992; p 75.

(9) Dua, S.; Blanksby, S. J.; Bowie, J. H. *Int. J. Mass Spectrom.* **2000**, *195/196*, 45.

(10) Brown, R. D.; Eastwood, F. W.; Elmes, P. S.; Godfrey, P. D. *J. Am. Chem. Soc*. **1983**, *105*, 6496.

(11) Brown, R. D.; McNaughton, D. A.; Dyall, K. G. *Chem. Phys.* **1988**, *119*, 189. Maclagan, R. G. A. R.; Sudkeaw, P. *J. Chem. Soc., Faraday Trans*. **1993**, *89*, 3325.

(12) Moazzen-Ahmalsi, M.; Zerbetto, F. *J. Chem. Phys.* **1995,** *103*, 6343.

(13) Botschwina, P.; Flügge, J.; Sebald, P. *J. Phys. Chem.* **1995**, *99*, 9755.

(14) Ogata, T.; Ohshima, Y.; Endo, Y. *J. Am. Chem. Soc.* **1995**, *117*, 3593.

(15) Ohshima, Y.; Endo, Y.; Ogata, T. *J. Chem. Phys.* **1995**, *102*, 1493.

(16) Oakes, J. M.; Ellison, G. B. *Tetrahedron* **1986**, *42*, 6263.

(17) Brown, R. D.; Godfrey, P. D.; Elmes, P. S.; Podler, M.; Tack, L. M. *J. Am. Chem. Soc.* **1985**, *107,* 4112.

(18) Ewing, D. W. *J. Am. Chem. Soc.* **1989**, *111*, 8809.

(19) Petrie, S.; Bettens, R. P. A.; Freeman, C. G.; McEwan, M. J. *Mon. Not. R. Astron. Soc.* **1993**, *264*, 862. Petrie, S.; Bettens, R. P. A.; Freeman, C. G.; McEwan, M. J. *J. Phys. Chem.* **1993**, *97*, 13673.

(20) Petrie, S.; Bettens, R. P. A.; Freeman, C. G.; McEwan, M. J. *J. Phys. Chem.* **1993**, *97*, 13673.

(21) Maclagan, R. G. A.; McEwan, M. J.; Scott, G. B. *Chem. Phys. Lett.* **1995**, *240*, 185.

(22) Ekern, S.; Szczepanski, J.; Vale, M. *J. Phys. Chem.* **1996**, *100*, 16109.

(23) Turner, B. E.; Zuirys, L. M. Interstellar Molecules and Astrochemistry. In *Galactic and Extragalactic Radio Astronomy*; Verschuur, G. L.; Kellerman, K. I., Eds.; Springer Verlag: Berlin, 1988.

(24) A reviewer has suggested that if C_3HO^+ captures an electron in the stellar environment, then the initially formed $C_3HO^\bullet$ will decompose to C_3O and $H^\bullet$. This process is endothermic by 66 kcal mol^{-1} (see Table 3), so the stability of $C_3HO^\bullet$ will depend on the energy of the captured electron.

(25) DePuy, C. H.; Bierbaum, V. M.; Flippin, L. A.; Grabowski, J. J.; King, G. K.; Schmitt, R. J.; Sullivan, S. A. *J. Am. Chem. Soc.* **1980**, *102*, 5012. Klass, G.; Trenerry, V. C.; Sheldon, J. C.; Bowie, J. H. *Aust. J. Chem.* **1981**, *34*, 519.

(26) Stringer, M. G.; Bowie, J. H.; Holmes, J. L. *J. Am. Chem. Soc*. **1986**, *108*, 3888.

(27) Bowie, J. H.; Blumenthal, T. *J. Am. Chem. Soc.* **1975**, *97*, 2959. Szulejko, J. E.; Bowie, J. H.; Howe. I.; Beynon, J. H. *Int. J. Mass Spectrom. Ion Phys*. **1980**, *13*, 76.

(28) Bursey, M. M. *Mass Spectrom. Rev.* **1990**, *9*, 555.

(29) For an account of neutralization/reionization of negative ions, and definitions of nomenclature, see: Goldberg, N.; Schwarz, H. *Acc. Chem. Res.* **1994**, *27*, 347 and references therein.

(30) For an account of the application of the comparison of $^-NR^+$ and CR spectra of an anion, see: Schalley, C. A.; Hornung, G.; Schröder, D.; Schwarz, H. *Chem. Soc. Rev.* **1998**, *27*, 91.

(31) Becke, A. D. *J. Phys. Chem.* **1993**, *98*, 5648.

(32) Stevens, P. J.; Devlin, F. J.; Chablowski, C. F.; Frisch, M. J. *J. Phys. Chem.* **1994**, *98*, 11623.

(33) Frisch, M. J.; Trucks, G. W.; Schlegel, H. B.; Gill, P. M. W.; Johnson, B. G.; Robb, M. A.; Cheeseman, J. R.; Keith, T.; Petersen, G. A.; Montgomery, J. A.; Raghavachari, K.; Al- Laham, M. A.; Zakrzewski, V. G.; Ortiz, J. V.; Foresman, J. B.; Peng, C. Y.; Ayala, P. Y.; Chen, W.; Wong, M.; Andres, J. L.; Replogle, E.; Gomperts, R.; Martin, R. L.; Fox, D. J.; Binkley, J. S.; Defrees, D. J.; Baker, J.; Stewart, J. P.; Head-Gordon, M.; Gonzales, C.; Pople, J. A. *GAUSSIAN94*, Revision B 3 ed.; GAUSSIAN Inc.: Pittsburgh, PA, 1995.

(34) Wong, M. W. *Chem. Phys. Lett.* **1996**, *256*, 391.

(35) Blanksby, S. J.; Dua, S.; Bowie, J. H. *J. Phys. Chem.* **1999**, *103*, 5161.

(36) Cizek, J. *Adv. Chem. Phys.* **1969**, *14*, 35.

(37) Pople, J. A.; Krishnan, R.; Schlegel, H. B.; Binkley, J. S. *Int. J. Quantum Chem.* **1978**, *XIV*, 545.

(38) Hampel, C.; Peterson, K.; Werner, H.-J. *Chem. Phys. Lett.* **1992**, *190*, 1.

(39) Watts, J. D.; Gauss, J.; Bartlett, R. J. *J. Chem. Phys.* **1993**, *98*, 8718.

(40) Knowles, P.; Hampel, C.; Werner, H.-J. *J. Chem. Phys.* **1993**, *99*, 5219.

(41) Dunning, T. H. *J. Chem. Phys.* **1989**, *90*, 1007.

(42) Woon, D. E.; Dunning, T. H. *J. Chem. Phys.* **1993**, *98*, 1358.

(43) Danheiser, R. L.; Fink, D. M.; Okano, K.; Tsai, Y. M.; Szezepanski, S. W. *Org. Synth. Coll. Vol VIII* **1993**, 501.

(44) Breslow, R.; Pecorar, J.; Sugimoto, T. *Org. Synth. Coll. Vol VI* **1981**, 361.

(45) Tomasic, Z. A.; Scuseria, G. E. *J. Phys.Chem.* **1991**, *95*, 6905.

(46) Cooksy, A. L.; Watson, J. K. G.; Gottlieb, C. A.; Thaddeus, P. *Astrophys. J.* **1992**, *386*, L27.

(47) Wang, H.; Cooksy, A. L. *Chem. Phys.* **1996**, *213*, 139.

(48) For example, the following geometries of $HC^3C^2C^1O$ have been reported: (i) at the TZ2P−SCF level of theory:[45] HC^3 (1.07 Å), C^3C^2 (1.26), C^2C^1 (1.29), C^1O (1.13), HC^3C^2 (137°), $C^3C^2C^1$ (159), C^2C^1O (175), and (ii) at the QCISD/6-311G (d, p) level of theory:[47] HC^3 (1.07 Å), C^3C^2 (1.21), C^2C^1 (1.44), C^1O (1.18), HC^3C^2 (177), $C^3C^2C^1$ (169), C^2C^1O (133).

(49) A reviewer has asked us to comment on the accuracy of the calculation at this level. We are unable to compare the calculated value of the electron affinity of C_3HO with an experimental value since the experimental value has not been reported. However we have compared calculated values of electron affinities at this level of theory with experimental values in previous studies, viz for C_3H (calculated 1.79 eV, experimental 1.86 eV)[50] and C_2CH_2 (calculated 1.67 eV, experimental 1.79 eV).[51]

(50) Blanksby, S. J.; Dua, S.; Bowie, J. H. *J. Phys. Chem. A.* **1999**, *103*, 5161.

(51) Blanksby, S. J.; Dua, S.; Bowie, J. H.; Schröder. D.; Schwarz, H. *J. Phys. Chem. A* **1998**, *102*, 9949.

(52) Noest, A. J.; Nibbering, N. M. M. *J. Am. Chem. Soc.* **1980**, *102*, 6427.

(53) Thermochemical data from the NIST Chemistry Web book. http://webbook.nist.gov.

(54) Goode, G. C.; Jennings, K. R. *Adv. Mass Spectrom.* **1974**, *6*, 797.

(55) Dua, S.; Sheldon, J. C.; Bowie, J. H. *Rapid Commun. Mass Spectrom.* **1994**, *8*, 533.

(56) For discussions of Franck−Condon overlap of potential surfaces of neutral and charged systems, see: Hornung, G.; Schalley, C. A.; Dieterle, M.; Schröder, D.; Schwarz, H. *Chem. Eur. J.* **1997**, *3*, 1866. Schalley, C. A.; Hornung, G.; Schröder, D.; Schwarz, H. *Chem. Eur. J.* **1997**, *3*, 1866.

(57) There are two stable forms of HC_3O^+. The data listed in Table 2 are for the ground state ($^1\Sigma$) HC_3O^+. There is also a triplet $^3A'$ state 80.3 kcal mol^{-1} less stable than the ground state.

(58) Nelson, C. C.; McCloskey, J. A. *J. Am. Soc. Mass Spectrom*. **1994**, *5*, 339.

(59) Holmes, J. L. *Org. Mass Spectrom*. **1985**, *20*, 169.

(60) Dheandhanco, S.; Forte, L.; Fox, A.; Bohme, D. K. *Can. J. Chem.* **1986**, *64*, 641.

(61) Polce, M. J.; Beranova, S.; Nold, M. J.; Wesdemiotis, C. *J. Mass Spectrom*. **1996**, *32*, 1073.

(62) Petrie, S.; Bettens, R. P. A.; McEwan, C. G. *J. Phys. Chem.* **1993**, *97*, 13673.

(63) http://webbook.nist.gov/chemistry.

(64) Ikuda, S. *J. Chem. Phys.* **1997**, *106*, 4536.

(65) Raksit, A. B.; Bohme, D. K. *Int. J. Mass Spectrom. Ion Phys.* **1983**, *49*, 275.

(66) Hevko, J. M.; Dua, S.; Bowie, J. H.; Taylor, M. S. *J. Chem. Soc., Perkin Trans. 2* **1999**, 457.

(67) Gilbert, R. G.; Smith, S. C. *Theory of Unimolecular and Recombination Reactions*; Blackwell Scientific: Cambridge, U.K., 1990. Scott, A. P.; Radom, L. *J. Phys. Chem.* **1996**, *100*, 16502.

(68) Although radiative processes of cations have not been specifically reported for NR processes, such processes are quite common for cations. See, e.g.: Mitzner, R.; Campbell, E. E. B. *J. Chem. Phys.* **1995**, *103*, 2445. Ho, Y.-P.; Yang, Y.-C.; Klippenstein, S. J.; Dunbar, R. C. *J. Phys. Chem.* **1995**, *99*, 12115. Hansen, K.; Campbell, E. E. B. *J. Chem. Phys.* **1996**, *104*, 5012.